INTERNATIONAL JOURNAL OF HYDROGEN ENERGY 36 (2011) 13621–13631

Available at www.sciencedirect.com

ScienceDirect

journal homepage: www.elsevier.com/locate/he

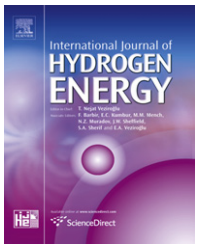

Modeling and simulation of absorption–desorption cyclic processes for hydrogen storage-compression using metal hydrides

B.A. Talagañis [a,*], G.O. Meyer [b], P.A. Aguirre [a]

[a] Instituto de desarrollo y diseño (INGAR), Consejo Nacional de Investigaciones Científicas y Técnicas (CONICET), Avellaneda 3657, S3002GJC Santa Fe, Argentina

[b] Instituto Balseiro, Universidad Nacional de Cuyo, CONICET, Comisión Nacional de Energía Atómica, Centro Atómico Bariloche, Av. Bustillo 9500, S.C. de Bariloche, Argentina

ARTICLE INFO

Article history:
Received 21 March 2011
Received in revised form
15 July 2011
Accepted 22 July 2011
Available online 26 August 2011

Keywords:
Modeling
Simulation
Hydrides
Hydrogen thermal compression
Storage

ABSTRACT

This work is aimed to develop and analyze reduced and simplified lumped models of cyclic processes for hydrogen storage and thermal compression using metal hydrides. Rigorous models involve several thousands of variables whereas reduced models we are interested in involve only several tens of variables. The models here presented reproduce the main dynamic behavior of rigorous models and experimental data found in the literature. Furthermore, the main tradeoffs arisen in process design are well described with these models, which is always an objective of optimal process design.

In the first part of the work, a simplified lumped model is developed and validated by comparing the simulations outcome with numerical results and experimental measurements obtained from the literature for absorption and desorption individual processes. Our model is then used to simulate the process behavior using real parameters and constraints required by continuous recovery and compression systems such as those found in the metal treatment industry. The simulation results are used to improve the process performance by adjusting some key parameters of the system. These results are also used to perform a sensitivity analysis, i.e. evaluate the storage/compression system behavior when introducing variations to parameters such as operating conditions, reactor design, and material properties.

Finally, we further reduce the model by considering that the inlet and outlet hydrogen flow is approximately constant. This particular specification is usually required by continuous processes in the metal treatment industry where hydrogen flow must remain constant. This requirement allows considering reaction rate as a constant. The constant reaction rate constraint allows integrating the ordinary differential equations; hence the system no longer has differential and algebraic equations but just algebraic equations. As a consequence of the simplification, the number of equations to be solved is reduced from over 15,000 to less than 50, maintaining an excellent match in the results.

* *Corresponding author*. Tel.: +54 342 4555229; fax: +54 342 4553439.
E-mail addresses: andrestalaganis@yahoo.com.ar, andrestalaganis@santafe-conicet.gov.ar (B.A. Talagañis), gmeyer@cab.cnea.gov.ar (G.O. Meyer), paguir@santafe-conicet.gov.ar (P.A. Aguirre).

0360-3199/$ – see front matter
doi:10.1016/j.ijhydene.2011.07.139

Nomenclature

t	time, s
m	mass, g or kg
f	hydrogen flow, g s^{-1} or kg s^{-1}
r	reaction rate, g_{MH} g_S^{-1} s^{-1}
T	temperature, K
P	pressure, bar
A	heat interchange area, m^2
V	volume, m^3
U	overall heat transfer coefficient, W m^{-2} K^{-1}
λ	thermal conductivity, W m^{-1} K^{-1}
h	conductance, W m^{-2} K^{-1}
ΔH	enthalpy, J mol^{-1}
ΔS	entropy, J mol^{-1} K^{-1}
C	kinetic constant, s^{-1}
E	activation energy, J mol^{-1}
c_p	specific heat, J g^{-1} K^{-1} or J kg^{-1} K^{-1}
R	universal gas constant, J mol^{-1} K^{-1}
wt%	hydrogenation capacity in weight percent
MW	molecular weight, g mol^{-1} or kg mol^{-1}
SC	stoichiometric coefficient
sl	plateau slope coefficient
ε	porosity

Subscripts

a	absorption
d	desorption
heat	heating
cool	cooling
eq	equilibrium
H_2	hydrogen
MH	metal hydride
Al	Aluminum
S	solid
g	gas
w	refrigerating/heating water
out	outlet
in	inlet
ini	initial
fin	final

1. Introduction

Over the last two decades, extensive research has been carried out on hydride forming materials as a result of their wide applications concerning hydrogen technology such as storage, heat pumps, thermal compression, and purification, among others [1]. Developments in metal hydride technology show that metal hydrides provide the possibility of storing hydrogen with several advantages over the conventional methods such as liquidification and gas compression, and also with high safety standards for both mobile and stationary applications. The interest is focused on materials where hydriding process takes place at relatively low pressure and temperature. By supplying heat or reducing pressure, absorbed hydrogen can be easily extracted from the hydride. It is also possible to increase the gas pressure by increasing material temperature during desorption. Nevertheless, the efficient use of metal hydride beds for proficient operations in both hydrogen absorption and desorption requires the analysis of the complex heat and mass transfer procedure inside the hydride bed. In that way, mathematical modeling of hydrogen storage in metal hydride beds has received considerable attention in recent years and several numerical models describing energy and mass transfer processes are available in the literature. Some authors consider phenomena as a one dimensional problem [2,3] and others take into account the two dimensional effects. The one dimensional model used by Mayer et al. [3] assumes that gas and solid temperatures are equal and that gas pressure is constant in the reactor. They also developed a widely used kinetic expression for absorption and desorption chemical reactions. Nasrallah et al. have published various papers [4–8] describing heat and mass transfer in a reactor. They used their model to study the validity of various simplifying assumptions used by different authors, for example considering thermal equilibrium between gas and solid. They have also demonstrated that convection is not significant in hydriding processes, and that radiative heat transfer is negligible in the $LaNi_5$–H_2 system. Recently, Demircan et al. [9] presented an experimental and theoretical analysis of the hydriding process. They concluded that hydriding time is mainly affected by heat removal from the bed. Consequently, hydriding time could be significantly reduced by using a bed design which provides a larger heat transfer area.

There exist various technological applications using metal hydrides, namely heat pumps, hydrogen storage, thermal compression, and purification. However, the application concerning hydrogen storage is by far the most studied case; and several theoretical and experimental studies have been carried out on the various aspects of hydrogen storage processes. When analyzing the use of metal hydrides for heat pumps and hydrogen thermal compression, it is important to study the coupling of the four stages of a complete cycle: 1) hydrogen absorption along with cooling, 2) material heating, 3) hydrogen desorption along with heating, and finally 4) material refrigeration to reach the cycle initial conditions. The literature provides many works dealing with these stages in heat pumps and cooling systems [10–13]. In this work, the objective is to study theoretically the coupling of the four stages applied to a hydrogen thermal compression process in order to develop a simple lumped model which allows the process simulation and, also, to develop a reduced model for optimal process design.

In a lumped model the equations describing chemical exchange and transport are ordinary differential equations rather than partial differential equations. Hence all the

variables have a unique value, a mean value, in the reactor geometry, i.e. the value of the variables is independent of the position (x,y,z) in the reactor.

The model equations allow two possibilities for analysis: the evaluation of process performance with established parameters, or the optimal process synthesis, design, and operation by analyzing the influence of different parameters on system performance. In the present work, design parameters are first fixed and hydrogen storage/compression process performance is evaluated in different scenarios.

In the first part of this study, our lumped model is validated by comparing its results with numerical and experimental works described in the literature. Numerical evaluation of time evolution of key variables such as hydrogen storage capacity and average bed temperature is reported; and consistency between these results and those available in the literature is discussed. Then, the hydrogen storage/compression process is simulated with real parameters and constraints required by usual processes in the metal treatment industry. These results are used to improve the process performance by adjusting key parameters such as the required mass of hydride forming material. Simulations results are also used to perform a sensitivity analysis of the process; i.e. evaluate the storage/compression system behavior when introducing variations to parameters such as operating conditions, reactor design, and material properties.

Finally, a particular specification usually required by continuous processes in the metal treatment industry is added: approximately constant inlet and outlet hydrogen flow. This specification allows considering reaction rate as a constant. This simplification allows reducing the number of equations from over 15,000 equations to less than 50 equations. Consequently, the computational resources needed to perform the simulation are significantly reduced while the numerical results match those from the lumped model.

2. Mathematical model

A cylindrical reactor filled with porous $LaNi_5$ is considered. The reactor is cooled (heated) during absorption (desorption) by flowing water on its external surface. The developed mathematical model is based on the following assumptions:

- Temperature and pressure are uniform in the reactor (lumped model).
- Ideal gas law holds in the gas phase.
- Porous medium is homogeneous and isotropic.
- Radiative heat transfer is negligible.
- Inlet/outlet hydrogen pressure is constant.
- Volume of gas phase, solid phase and reactor are constant.
- Physical properties of the hydride bed are independent of temperature and hydrogen pressure.
- Outlet gas temperature and pressure are equal to those of gas inside the reactor.

A model considering temperature and pressure variation inside the reactor must be represented using partial differential equations. The assumption of uniform temperature and pressure allows simplifying the model. As a result, the equations describing mass and energy balances are ordinary differential equations rather than partial differential equations. Hence, the simplification turns the system of partial differential equations into a system of just ordinary differential equations. Actually, temperature and pressure values at different positions inside the reactor are not uniform. If the model is intended to represent temperature and pressure distribution inside the reactor, then it is not possible to make this assumption. In our analysis, however, is not necessary to obtain this distribution. Reaction evolution is properly represented by obtaining an average temperature and pressure value in the reactor. Then, average temperature and composition are used in the mass and energy balances. Calculations of bed and gas properties are averaged too. Calculations for the average heat transfer coefficients involve some considerations, which are explained below.

Considering these assumptions, the equations governing heat and mass transfer in the metal–hydrogen reactor are the following.

2.1. Gaseous hydrogen mass balance

Hydrogen mass conservation equation is:

For absorption:

$$\frac{dm_{H_2g}}{dt} = f_{inH_2} - rm_S \frac{MW_{H_2} SC}{MW_{MH}} \tag{1}$$

For desorption:

$$\frac{dm_{H_2g}}{dt} = -f_{outH_2} - rm_S \frac{MW_{H_2} SC}{MW_{MH}} \tag{2}$$

2.2. Metal hydride mass balance

Solid mass conservation equation either for absorption or desorption is:

$$\frac{dm_{MH}}{dt} = rm_S \tag{3}$$

2.3. Energy balance equation

One usual assumption in most studies is considering gas phase temperature equal to solid phase temperature. Then, a single energy equation is sufficient to determine temperature in the reactor:

For absorption:

$$(m_{H_2g} c_{pH_2} + m_S c_{pS}) \frac{dT}{dt} = f_{inH_2} c_{pH_2} (T_{in} - T) + AU(T_{wa} - T) - \Delta H_a rm_S \frac{SC}{MW_{MH}} \tag{4}$$

For desorption:

$$(m_{H_2g} c_{pH_2} + m_S c_{pS}) \frac{dT}{dt} = AU(T_{wd} - T) + \Delta H_d rm_S \frac{SC}{MW_{MH}} \tag{5}$$

As mentioned above, overall heat transfer coefficient (U) needs some considerations. It involves thermal conductivity of the metal hydride bed (λ) and conductance between the external face of the reactor and the cooling/heating fluid (h):

$$\frac{1}{U}=\frac{1}{h}+\frac{1}{\lambda}$$

For a cylindrical reactor with radius << length, the term $1/\lambda$ is obtained by calculating a volume averaged conductance (h_{av}) as follows:

$$\frac{1}{\lambda}=\frac{1}{h_{av}}=\frac{\sum V_i}{\sum h_i V_i}$$

Where V_i and h_i are volume and conductance of layer i respectively (see Fig. 1).

$$V_i=\pi\left(\text{radius}_i^2-\text{radius}_{i-1}^2\right)*\text{length}$$

$$h_i=\frac{\lambda}{r_i\ln\left(\frac{\text{radius}_i}{\text{radius}_{i-1}}\right)}$$

2.4. Reaction kinetics

Several expressions for sorption reaction rate in metal hydrides are available in the literature. These expressions are functions of various modeling parameters, namely hydrogen pressure, temperature and concentration at a given time. One major problem in finding a general and valid correlation is that the rate constant may change during the reaction. This happens because the reaction between hydrogen and metal consists of several partial reactions on the surface and in the bulk material [14,15]. Extensive studies have led to different conclusions on the type of kinetics and controlling mechanisms being involved. However, there exists a widely accepted model which is successfully used for the case of $LaNi_5$–H_2 system [3–6,8,9,16,17]:

For absorption:

$$r=C_a e^{-E_a/RT}\ln\left(\frac{P_a}{P_{eq}}\right)\left(1-\frac{m_{MH}}{m_S}\right) \quad (6)$$

For desorption:

$$r=C_d e^{-E_d/RT}\frac{(P_d-P_{eq})}{P_{eq}}\left(\frac{m_{MH}}{m_S}\right) \quad (7)$$

Where E_a and E_d are activation energy for absorption and desorption respectively; C_a and C_d are kinetic constants; P_{eq} is equilibrium pressure (see Section 2.5); m_S is a constant which represents solid material mass in the system; and m_{MH} is a variable that represents the current metal hydride mass, and thus it represents the reaction progress.

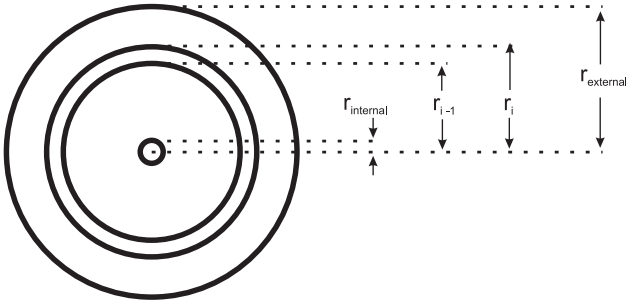

Fig. 1 – Schematic draw of reactor cross-section.

2.5. Equilibrium pressure

Pressure composition isotherms, generally called PCIs, show the dependence of equilibrium pressure on temperature and also on the hydrogen to metal ratio H/M. In order to model PCI as a temperature and H/M function, many attempts have been made to fit the experimental data to a polynomial of *n*th degree. For the case of $LaNi_5$, available 5th and 9th degree polynomial fits are given in [4,5] and [7], respectively. However, this way of modeling PCI curve should not be used to model equilibrium pressure (P_{eq}) of the hydriding reaction. In low- and high-concentration regions (the nonlinear regions to be represented by the polynomial fit), processes are related to hydrogen diffusion in the solid solution and not to the exothermic hydriding reaction. Thus, using the polynomial expression to model equilibrium pressure would lead to an overestimated value of reaction kinetics and to a subsequent overestimation of reactor temperature. A better way of modeling equilibrium pressure consists of using van't Hoff equation [3,9,17–19]. According to van't Hoff relation, plateau pressure of an ideal hydride only depends on temperature. Nonetheless, a constant slope term is usually added to approximate real material behavior [20]. Equilibrium pressure is then a function of temperature and hydrogen concentration, and can be represented as follows:

For absorption:

$$P_{eq}=e^{\left(\frac{\Delta H_a}{RT}-\frac{\Delta S_a}{R}+sl\left(\frac{m_{MH}}{m_S}-0.5\right)\right)}P_0 \quad (8)$$

For desorption:

$$P_{eq}=e^{\left(-\frac{\Delta H_d}{RT}+\frac{\Delta S_d}{R}+sl\left(\frac{m_{MH}}{m_S}-0.5\right)\right)}P_0 \quad (9)$$

2.6. Auxiliary expressions

Ideal gases state equation:

$$m_{H_2g}=\frac{PV_g}{RT}MW_{H_2} \quad (10)$$

Hydrogenation capacity in weight percent:

$$wt\%=\frac{m_{MH}}{m_S}\frac{MW_{H_2}SC}{MW_{MH}}100=\frac{m_{MH}}{m_S}wt\%_{max} \quad (11)$$

2.7. Initial conditions and discretization

The reactor is cooled/heated by flowing water on its external surface. Cooling/heating water temperature is assumed to be constant. Reactor temperature at the initial time of the absorption stage is equal to the cooling water temperature: $T_{a\ (initial)}=T_{wa}$. Reactor temperature at the initial time of the desorption stage is equal to the heating water temperature: $T_{d\ (initial)}=T_{wd}$. The values used in the simulations are shown in Tables 1 and 2. Additional constraints link the stages of the cycle: the final temperature value of each stage is equal to the initial temperature value of the next stage; i.e. $T_{a\ (final)}=T_{heat\ (initial)}$, $T_{heat\ (final)}=T_{d\ (initial)}$, $T_{d\ (final)}=T_{cool\ (initial)}$, $T_{cool\ (final)}=T_{a\ (initial)}$. Initial metal hydride mass is $m_{MH\ (initial)}=0$ for absorption, and $m_{MH\ (initial)}=m_S$ for desorption. For simulation case

Table 1 – - Parameters used in computations.

Parameter	Laurencelle et al. small reactor	Laurencelle et al. large reactor	Muthukumar et al.	Units
Material	$LaNi_5$	$LaNi_5$	$MmNi_{4.6}Al_{0.4}$	
A	5.0×10^{-4}	3.0×10^{-3}	3.82×10^{-2}	m^2
V_g	4.4×10^{-7}	4.8×10^{-6}	6.16×10^{-5}	$m^3_{H_2}$
Length	0.0254	0.0762	0.45	m
h	100	3000	1000	$W\,m^{-2}\,K^{-1}$
λ	0.21	11.1	1.6	$W\,m^{-1}\,K^{-1}$
U	80	2500	672	$W\,m^{-2}\,K^{-1}$
m_s	1	25	500	gs
P_a	6	12.7	10- 20–30	bar
P_d	0.068	0.086		bar
P_o	1	1	1	bar
T_{wa}	296	323	298	K
T_{wd}	296	323		K
T_{in}	290	290	313	K
ΔH_a	−30,478	−30,478	−28,000	$J\,mol^{-1}_{H_2}$
ΔH_d	30,800	30,800		$J\,mol^{-1}_{H_2}$
ΔS_a	−108	−108	−107.2	$J\,mol^{-1}_{H_2}\,K^{-1}$
ΔS_d	108	108		$J\,mol^{-1}_{H_2}\,K^{-1}$
E_a	21,170	21,170	21,170	$J\,mol^{-1}_{H_2}$
E_d	16,420	16,420		$J\,mol^{-1}_{H_2}$
C_a	59.2	59.2	75	s^{-1}
C_d	9.6	9.6		s^{-1}
C_{pH_2}	14.3	14.3	14.3	$J\,g^{-1}_{H_2}\,K^{-1}$
C_{pS}	0.355	0.355	0.419	$J\,g^{-1}_{S}\,K^{-1}$
C_{pAl}		0.963		$J\,g^{-1}_{Al}\,K^{-1}$
m_{Al}		18		g_{Al}
R	8.314	8.314	8.314	$J\,mol^{-1}_{H_2}\,K^{-1}$
MW_{Hz}	2	2	2	$g_{H_2}\,mol^{-1}_{H_2}$
MW_{MH}	432	432	421	$g_{MH}\,mol^{-1}_{MH}$
SC	2.76	2.76	3	$mol_{H_2}\,mol^{-1}_{MH}$
$wt\%_{max}$	1.28	1.28	1.42	
ε_{HM}	0.55	0.55	0.5	
ε_{Al}	1	0.91		
sl	0.13	0.13		

number 2 (Section 4): $m_{MH\ (initial)} = 27$ kg for the absorption stage and $m_{MH\ (initial)} = 98$ kg for the desorption stage. Hydride mass at the end of the absorption stage is equal to hydride mass at the beginning of the desorption stage and vice versa.

The trapezoidal method was used to obtain approximate solutions to the ordinary differential Eqs. (1)–(5). Trapezoidal method is an implicit method for numerically solving initial value problems for ordinary differential equations (ODE). It provides an approximate step-by-step solution in discrete increments across the integration interval. In fact, it produces a discrete sample of approximate values of the solution function. Specifically, from an approximate solution value y_k at time t_k for an ODE $y' = f(t, y)$, the trapezoidal method provides an approximate solution $y(t_{k+1})$ at time $t_{k+1} = t_k + h_k$ by solving the implicit equation $y_{k+1} = y_k + h_k\,[f(t_k, y_k) + f(t_{k+1}, y_{k+1})]/2$ for y_{k+1}.

1000 discretization steps were selected for each ODE of the model. Hence, the resulting model consists of a system of 15,020 equations. The amount of discretization steps arose from the system's error control analysis.

3. Model validation

The differential and algebraic equations system presented in the previous section is numerically solved by using GAMS (General Algebraic Modeling System) [21]. The generalized reduced gradient algorithm CONOPT3 is selected to solve the nonlinear programming (NLP) problem.

For this model validation, our numerical results were compared to reported data in the literature. First, a reactor and hydride forming material were considered with the same characteristics and operating conditions as those in the experimental and numerical work by Laurencelle et al. [20]. Total absorbed/desorbed mass time evolution and average temperature inside the reactor during absorption and desorption in both works were compared. Simulation parameters are summarized in Table 1. Hydrogenation capacity is represented by its reversible part and plateau curvature is neglected. In order to consider only the reversible part of the plateau in the simulations, the stoichiometric coefficient of reaction is decreased from 3 to 2.76. The kinetic parameters values were used in several models [3–6,8,9,16,17].

Experimental and numerical results of measurements and simulations for two different reactors were compared. The first one, called "small reactor", is made of stainless steel, contains 1 g of $LaNi_5$ and it is equipped with no heat exchanger. The second one, identified as "large reactor", contains 25 g of $LaNi_5$ and 18 g of aluminum foam which improves heat transfer rate. Heat transfer in this reactor is

Table 2 – Parameters used in simulation cases 1 and 2.

	Parameter	Case 1	Case 2	Units	Reference
	Material	$LaNi_5$	$LaNi_5$		
Hydride physicochemical properties	ΔH_a	−30,478	−30,478	$J\,mol_{H_2}^{-1}$	[20,24]
	ΔH_d	30,800	30,800	$J\,mol_{H_2}^{-1}$	Presi dal riferimento 24
	ΔS_a	−108	−108	$J\,mol_{H_2}^{-1}\,K^{-1}$	
	ΔS_d	108	108	$J\,mol_{H_2}^{-1}\,K^{-1}$	
	E_a	21,170	21,170	$J\,mol_{H_2}^{-1}$	[25]
	E_d	16,420	16,420	$J\,mol_{H_2}^{-1}$	NON disponibile
	C_a	59.2	59.2	s^{-1}	
	C_d	9.6	9.6	s^{-1}	
	c_{pS}	355	355	$J\,kg_S^{-1}\,K^{-1}$	[20]
	λ	0.66	0.66	$W\,m^{-1}\,K^{-1}$	[26]
	sl	0.13	0.13		[20]
	MW_{MH}	0.432	0.432	$kg_{MH}\,mol^{-1}{}_{MH}$	
	$wt\%_{max}$	1.39	1.39		Presi dal riferimento 20
Reactor design	V_g	0.0172	0.013	$m^3_{H_2}$	
	A	5.4	4.147	m^2	
	h	500	500	$W\,m^{-2}\,K^{-1}$	Media tra 1.2 e 0.12 del riferimento 26
	U	243	243	$W\,m^{-2}\,K^{-1}$	
	m_s	143	109.3	kg_S	
	length	1	1	m	
	n° of tubes	68	52		
	diameter	0.0254	0.0254	m	
Operating conditions	P_a	5	5	bar	
	P_d	6	6	bar	
	T_{wa}	298	298	K	
	T_{wd}	353	353	K	
	T_{in}	290	290	K	
	t_a	1440	720	s	
	t_{heat}	360	180	s	
	t_d	1440	720	s	
	t_{cool}	360	180	s	
Other parameters	c_{pH_2}	14,300	14,300	$J\,kg_{H_2}^{-1}\,K^{-1}$	
	MW_{H_2}	0.002	0.002	$kg_{H_2}\,mol_{H_2}^{-1}$	
	R	8.314	8.314	$J\,mol_{H_2}^{-1}\,K^{-1}$	
	SC	3	3	$mol_{H_2}\,mol_{MH}^{-1}$	
	P_0	1	1	bar	
	ε	0.5	0.5		

also improved by a water circulation loop. For further information on experimental details see [20]. As the "large reactor" includes aluminum foam, the energy balance equation for absorption (4) and desorption (5) must be adjusted as follows.

For absorption:

$$(m_{H_2g}c_{pH_2}+m_Sc_{pS}+m_{Al}c_{pAl})\frac{dT}{dt}=f_{inH_2}c_{pH_2}(T_{in}-T)+AU(T_{wa}-T)-\Delta H_a r m_S\frac{SC}{MW_{MH}}$$

For desorption:

$$(m_{H_2g}c_{pH_2}+m_Sc_{pS}+m_{Al}c_{pAl})\frac{dT}{dt}=AU(T_{wd}-T)+\Delta H_d r m_S\frac{SC}{MW_{MH}}$$

Comparison between the numerical results provided by our work and those measured and modeled by Laurencelle are shown in Figs. 2 and 3. Fig. 2 shows hydrogen absorption and desorption for both reactors; and Fig. 3 shows the corresponding temperature profiles. As our lumped model gives a uniform temperature value inside the reactor, this result was compared to the averaged temperature numerically obtained by Laurencelle et al. As it can be seen, there exists a perfect match between our results and those reported by Laurencelle.

It should be noted that no parameter had to be adjusted in our model to approximate the published data. In fact, all values were taken from the literature and calculated according to the described equations.

As a second model validation, our results were also compared to the experimental measurements and numerical simulations carried out by Muthukumar et al. [22,23]. A reactor and hydride forming material were considered with the same characteristics and operating conditions as those in the work by Muthukumar. These parameters are summarized in Table 1. For the correct simulation of absorption equilibrium pressure; Eq. (8) of our model is replaced by the equilibrium pressure equation used by Muthukumar:

$$P_{eq}=e^{\left(\frac{\Delta H_a}{RT}-\frac{\Delta S_a}{R}+(\varphi_S+\varphi_0)\tan\left(\pi\left(\frac{m_{MH}}{m_S}-0.5\right)+\frac{\varphi}{2}\right)\right)}P_0$$

where φ_s and φ are slope and hysteresis factor respectively and φ_0 is a constant. The value of these parameters for $MmNi_{4.6}Al_{0.4}$ are: $\varphi_s=0.35$, $\varphi=0.2$ and $\varphi_0=0.15$.

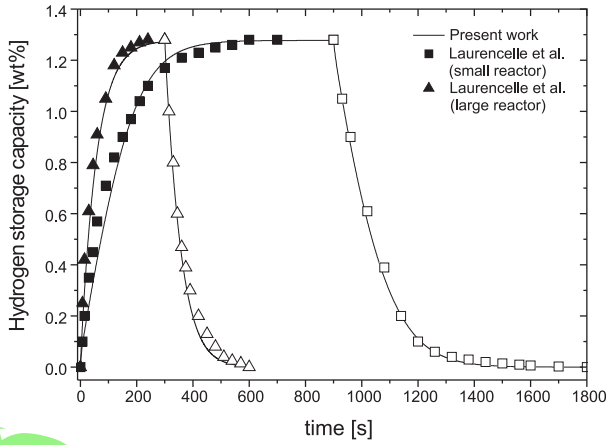

Fig. 2 – Validation of predicted hydrogen storage capacity profiles. Full symbols correspond to absorption and hollow symbols to desorption.

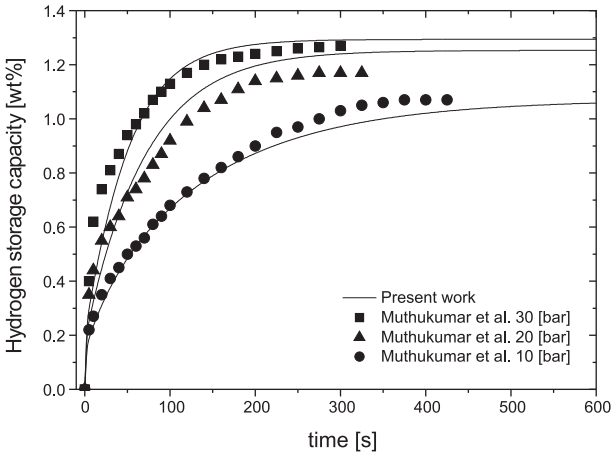

Fig. 4 – Validation of predicted hydrogen storage capacity profiles. The symbols correspond to the measurements performed by Muthukumar et al. [19], the full lines are the corresponding simulation results of our model.

Fig. 4 shows the comparison between our numerical results and the experimental measurements performed by Muthukumar et al. [23].

These curves show the absorbed hydrogen mass time evolution for three different system pressures: 10 (circles), 20 (triangles) and 30 (squares) bar. The system pressure remains constant throughout the whole sorption reaction. Although our results slightly overpredict the total absorbed mass value for the measurement at 20 bar, numerical results satisfactorily capture the physics of the hydriding processes.

4. Simulation results

In this section, our lumped model is used to simulate and improve the design of the hydrogen storage/compression process. This process must guarantee a fixed hydrogen production of 2 kg_{H_2}/h. $LaNi_5$ is selected as the hydride forming material for the process. This material has many advantages for this particular application: high cycling resistance, high gas impurities resistance, low plateau slope, and low hysteresis. The main disadvantage of $LaNi_5$-family hydrides is their low storage capacity. However, since this application is stationary, gravimetric density is not relevant. $LaNi_5$ hydrogen storage capacity is 1.39 wt%, and thus the required 2 kg_{H_2}/h production means that 143 kg_{MH}/h (0.03972 kg_{MH}/s) must be produced. This production level is a fixed parameter in the simulations.

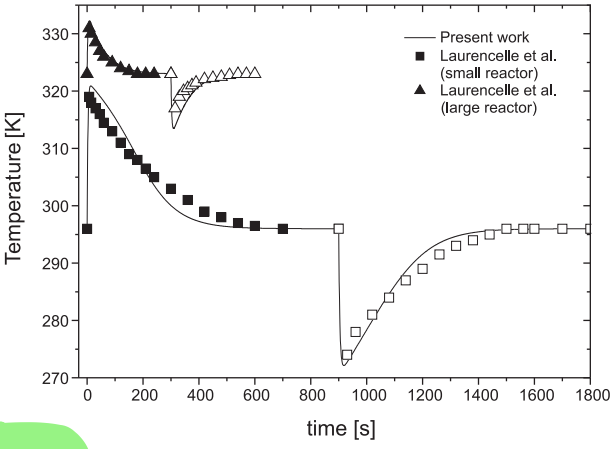

Fig. 3 – Validation of predicted temperature profiles. Full symbols correspond to absorption, hollow symbols to desorption.

Cooling and heating water temperatures are 298 and 353 K respectively. The inlet pressure corresponding to the absorption stage is 5 bar; and the required outlet pressure corresponding to the desorption stage is 6 bar.

Considering these requirements, and assuming that the material is absorbed and desorbed by above 99% of its capacity, a complete hydrogen storage/compression cycle takes approximately 1 h. Therefore, 143 kg of $LaNi_5$ are needed in order to satisfy the required production of 143 kg_{MH}/h. The 143 kg of $LaNi_5$ are located in a multi tubular reactor. This type of reactor is preferable due to the large amount of solid material that must be accommodated. The reactor shape is similar to a shell and tube heat exchanger where the hydride is placed inside the tubes, and the cooling/heating water flows on the outside. Each tube is modeled as a cylindrical reactor. Several calculations were performed to select the appropriate tube length and diameter. The calculations confirmed that several small diameter tubes are preferable in order to increase both inner conductance value and heat transfer area.

Two simulation cases are presented in this work. In the first case, the conditions explained in the previous paragraphs were simulated (cycle time 1 h, 143 kg $LaNi_5$ mass). For this scenario, 143 kg of hydride forming material were needed.

Since the hydride forming material ($LaNi_5$) is a key parameter because of its high cost, other process conditions were studied so as to use less amount of material, satisfying the required production level. After several simulations, the set of parameters corresponding to the second case were obtained. For this case, the cycle time was 0.5 h and only 109.3 kg of $LaNi_5$ were needed, attaining a 25% reduction in the amount of required material.

Reactor dimensions and other simulation parameters are detailed in Table 2. For both simulations, temperature initial conditions are the same: reactor temperature at the initial time of the absorption stage is equal to the temperature of the cooling water: $T_{a\ (initial)} = T_{wa}$. Reactor temperature at the initial time of the desorption stage is equal to the temperature of the heating water: $T_{d\ (initial)} = T_{w\ d}$. Final temperature value of each stage is equal to that of the initial temperature of the next stage; i.e. $T_{a\ (final)} = T_{heat\ (initial)}$, $T_{heat\ (final)} = T_{d\ (initial)}$, $T_{d\ (final)} = T_{cool\ (initial)}$, $T_{cool\ (final)} = T_{a\ (initial)}$.

Hydride mass initial condition for case 1 is $m_{MH\ (initial)} = 0$ for the absorption stage, and $m_{MH\ (initial)} = m_S$ for the desorption stage. Hydride mass initial condition for simulation case number 2 is: $m_{MH\ (initial)} = 27$ kg for the absorption stage and $m_{MH\ (initial)} = 98$ kg for the desorption stage. In both cases, the hydride mass at the end of the absorption stage is equal to the hydride mass at the beginning of the desorption stage and vice versa.

Fig. 5 shows the evolution of several key variables: hydride mass (5a), average bed temperature (5b), equilibrium pressure (5c) and reaction rate (5d) for the simulated cases.

As it can be seen, an approximately one-hour cycle time allows hydriding and dehydriding the solid material almost completely, satisfying production requirements (Fig. 5a, case 1).

Fig. 5b shows the evolution of average bed temperature throughout the cycle. Bed temperature at the beginning of the absorption stage is equal to the cooling water temperature. When the gaseous hydrogen flows into the reactor, the exothermic hydriding reaction begins. At the beginning of the absorption stage, reaction rate is high and so is the heat produced by the reaction (See Fig. 5d). Consequently, the cooling system is not able to evacuate all the heat produced by the chemical reaction and thus bed temperature increases. Increased bed temperature causes the corresponding increase in material equilibrium pressure (See Fig. 5c). As the reaction progresses, the reaction rate slows down. Heat production is then decreased and the refrigerating system can now dissipate the heat, and bed temperature diminishes. The same situation occurs during the desorption stage but in the opposite direction: desorption is an endothermic reaction and thus heating is required instead of cooling.

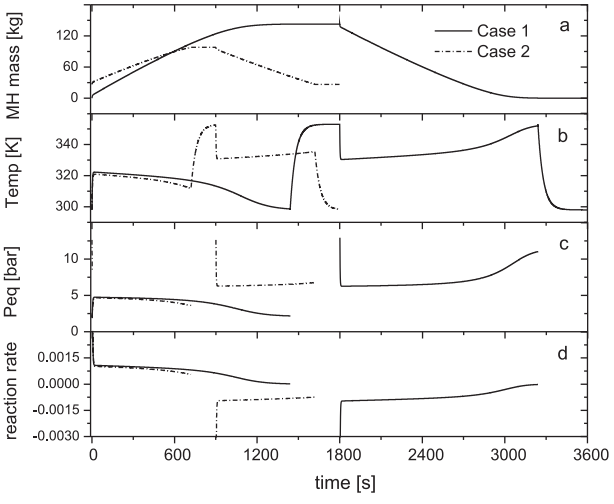

Fig. 5 – Variables evolution for simulations cases 1 and 2: hydride mass (a), average bed temperature (b), equilibrium pressure (c), reaction rate (d).

It is important to note that in case number 1, material is absorbed/desorbed above 99% of its capacity, whereas in case number 2 material is absorbed/desorbed only 65% (between 25% and 90%), showing the existing tradeoff between absorption and desorption stages. A complete material absorption or desorption are both inefficient situations because the reaction rate notably diminishes as the reaction progresses (see Fig. 5d). This suggests that further improvements can be made to reduce the required amount of material by using optimization strategies.

5. Sensitivity analysis

The effect of increasing or decreasing some model parameters of the simulation presented in Section 4 is now studied. As it was previously mentioned, the local solver GAMS/CONOPT3 is used to solve the nonlinear programming problem. After the resolution, one of the solver outputs is the marginal value for each variable and equation [27]. That is one of the advantages of implementing this optimization software and it will be explored here.

When an optimization problem is solved, a variable (i.e. the objective function) is minimized or maximized. Let y be the objective function. The marginal value of a variable x, also known as dual variable or Lagrangian multiplier, is defined as: $\partial y/\partial x$ evaluated at the optimal value. This partial derivative considers the explicit and implicit influence of variable x over variable y, given by the proper objective function definition as well as the model equations.

In the present work, the optimization software (GAMS/CONOPT3) is not used to solve an optimization problem but to simulate the system behavior by fixing as many variables as necessary so as to null the degrees of freedom of the system. When the optimization software is used for simulation, the objective function is a "dummy" function because the resulting evolution of variables is independent of the objective function. Nevertheless, the marginal value analysis can be still performed using as objective function the variable whose marginal values are to be found.

Marginal values are used to calculate relative marginal values (RMV), which are more suitable to evaluate the influence of the change at each variable over the whole process:

$$\mathrm{RMV} = \frac{\partial y}{\partial x}\frac{|x|}{y}$$

Table 3 shows the relative marginal values (RMV) of the main model parameters for the simulated scenario (case 2) presented in the previous section. The objective function for this case is to minimize the total mass of hydride forming material or "solid material" (m_S). Even though only results for this objective function are presented, the marginals for other objective functions such as maximizing production or desorption pressure were calculated, obtaining similar results.

Note that different types of parameters are studied: physicochemical properties of the hydride (ΔH, ΔS, E, C, sl, C_p),

Table 3 – Sensitivity analysis: relative marginal values for total hydride forming material mass.

Parameter	Type of parameter	Value	RMV
ΔS_d	Physicochemical	108	−48.3
T_{wd}	Operating	353	−43.5
ΔH_{dp}	Physicochemical	30,800	41.4
ΔS_a	Physicochemical	−108	−17.8
ΔH_{ap}	Physicochemical	−30,480	15.9
T_{wa}	Operating	298	12.4
P_d	Operating	6	3.77
A	Design	4.147	−3.31
ΔH_{dB}	Physicochemical	30,800	2.54
U_d	Design	243	−2.48
$T_{w\ heat}$	Operating	353	−2.20
E_d	Physicochemical	16,420	1.80
E_a	Physicochemical	21,170	1.74
P_a	Operating	5	−1.37
t_d	Operating	720	−1.05
ΔH_{aB}	Physicochemical	−30,480	−0.84
U_a	Design	243	−0.82
t_a	Operating	720	0.69
$T_{w\ cool}$	Operating	298	0.61
t_{cool}	Operating	180	0.43
t_{heat}	Operating	180	0.42
C_d	Physicochemical	9.6	−0.29
T_{in}	Operating	290	0.24
C_a	Physicochemical	59.2	−0.21
c_{pS}	Physicochemical	355	−0.12
sl	Physicochemical	0.13	0.01
U_{heat}	Design	243	−0.01
U_{cool}	Design	243	−0.004
V_g	Design	0.013	−0.0002

operating conditions (P, t, T_w, T_{in}) and reactor design parameters (U, A, V_g). All these parameters are defined as "variables" in GAMS models, and their values are fixed before solving the models. In this way, the solver computes the numerical derivative for the objective function and constraint with respect to these fixed variables and reports their values at optimality. Relative marginal values are arranged according to their absolute values. The positive sign of a relative marginal indicates that the objective function increases its value when the corresponding parameters are increased. On the contrary, a negative relative marginal indicates that increasing the parameter decreases the objective value. The marginal value shows how beneficial modifying a particular parameter can be. Then, if a parameter p is increased from its current value p^* by a small amount: Δp, the net change for the objective function y will be: $(\Delta p\ \partial y/\partial p)$ approximately.

As shown in Table 3, the reaction enthalpy and entropy as well as the cooling/heating water temperature during absorption and desorption are the most influential parameters over the total $LaNi_5$ mass used in the process. It would be profitable to increase the heating fluid temperature during desorption as well as decreasing the fluid temperature during absorption. However, as the marginals indicate, it would be much more profitable to try to increase it in the desorption stage than decreasing it during absorption.

As it can be seen in Table 3, we have used two different parameters with the same value for the absorption enthalpy ($\Delta H_{a\_}P$ and $\Delta H_{a\_}B$) and also two for the desorption enthalpy ($\Delta H_{d\_}P$ and $\Delta H_{d\_}B$). Enthalpies "_P" are used in the equilibrium pressure equations and enthalpies "_B" are used in the energy balance equations. In this way, the model computes the marginals for both cases. It is interesting to note that, while in the case of desorption enthalpy both marginals are positive (meaning that it would be profitable to decrease its values), in the case of absorption enthalpy one marginal is positive (ΔH_{ap}) and the other is negative (ΔH_{aB}). This shows that it would be beneficial for equilibrium pressure to diminish the reaction enthalpy (or increase its absolute value) because this would decrease equilibrium pressure; and, contrarily for the energy transfer, it would be beneficial to increase the reaction enthalpy (or decrease its absolute value) because it would generate less reaction heat.

Also, information about which parameters do not influence the objective can be obtained. For example, the little influence of kinetic constants over the objective function indicates that the reaction rate is more affected by heat transfer in the reactor than intrinsic material kinetics.

Reaction rate is mainly affected by the difference between system pressure and material equilibrium pressure (driving force of the reaction), and equilibrium pressure is given by system temperature, enthalpy and entropy. Hence, reaction rate is directly affected by reaction enthalpy and entropy as well as by cooling/heating fluid temperature.

The marginals of each cycle stage duration time indicate that absorption time (t_a), heating time (t_{heat}) and cooling time (t_{cool}) should be decreased while desorption time (t_d) should be increased, indicating a clear unbalance between absorption and desorption stages duration.

In that way, the effect of increasing or decreasing each parameter can be evaluated and considered according to the pursued objective.

6. Reduced model

As it was mentioned in the introduction, a further simplification of the model can be made considering constant hydrogen flow in the inlet and outlet streams. This specification is usually required by continuous processes where hydrogen flow is constant. This requirement is physically achieved by using mass flow controllers in the inlet and outlet hydrogen streams. The requirement of constant hydrogen flow means that reaction rate would be approximately constant. In order to maintain the reaction rate constant, the system pressure must be variable. Using the differential equations model, both cases considering variable and constant reaction rate are compared. In Fig. 6, the time evolution of several key variables is shown for both cases. Fig. 6a shows reaction rate; dashed line corresponds to the variable reaction rate case (constant system pressure, Fig. 6b) and solid line corresponds to the constant reaction rate case (variable system pressure, Fig. 6b). As it can be seen, when reaction rate is constant, temperature is lower during absorption and higher during desorption stage (Fig. 6c). Accordingly, equilibrium pressure behaves in the same way (Fig. 6d). It is important to note that the needed hydride forming material mass is higher when hydrogen flow is constant (see Fig. 6e). This occurs because system

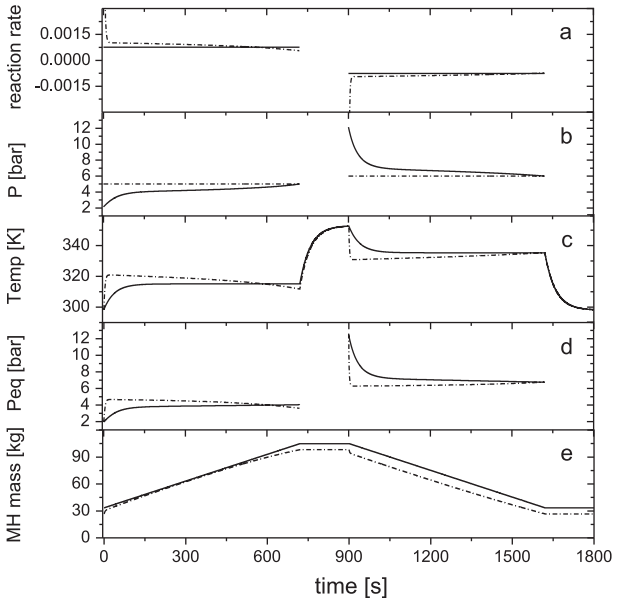

Fig. 6 – Comparison of simulation results using differential equations model with variable reaction rate (dashed line) and with constant reaction rate (solid line). Reaction rate (a), system pressure (b), average bed temperature (c), equilibrium pressure (d), hydride mass (e).

performance diminishes since reaction driving force – i.e. difference between system pressure and equilibrium pressure – is weaker. The driving force is weaker because the reaction rate control is accomplished by weakening the driving force.

Fixing the reaction rate allows simplifying the model. Since reaction rate is now a constant, the ordinary differential equations of the model can be integrated, thus the differential and algebraic equations system becomes a just algebraic equations system. The discretization procedure presented in Section 2.7 originates a large number of equations. For this reason, the model involving discretization of the differential equations consists of over 15,000 equations, while the model with only algebraic equations contains less than 50 equations. Consequently, the computational resources and time needed to perform the simulation are significantly reduced.

The algebraic and ordinary differential equations system can be simplified to obtain an algebraic equations system by adding the following assumptions:

- Absorption and desorption reaction rates are constant (hydrogen flow approximately constant).
- Hydrogen specific heat capacity is negligible as compared to solid material specific heat.
- Enthalpy introduced into the reactor by the hydrogen inlet flow is negligible.
- Gas pressure is variable according to the flow control system.

Considering these assumptions, the equations governing heat and mass transfer in the metal-hydrogen reactor are the following:

Hydrided fraction profile

For absorption:

$$\frac{m_{\mathrm{MH\ fin}}}{m_{\mathrm{S}}} = \frac{m_{\mathrm{MH\ ini}}}{m_{\mathrm{S}}} + r_{\mathrm{a}}\left(t_{\mathrm{fin}} - t_{\mathrm{ini}}\right) \tag{122}$$

For desorption:

$$\frac{m_{\mathrm{MH\ fin}}}{m_{\mathrm{S}}} = \frac{m_{\mathrm{MH\ ini}}}{m_{\mathrm{S}}} + r_{\mathrm{d}}\left(t_{\mathrm{fin}} - t_{\mathrm{ini}}\right) \tag{133}$$

Temperature profile

For absorption:

$$T_{fin} = T_{w\,a} - \frac{\Delta H_{\mathrm{a}} r_{\mathrm{a}} m_{\mathrm{S}} SC}{AUMW_{\mathrm{MH}}} + \left(T_{\mathrm{ini}} - T_{\mathrm{wa}} + \frac{\Delta H_{\mathrm{a}} r_{\mathrm{a}} m_{\mathrm{S}} SC}{AUMW_{\mathrm{MH}}}\right) e^{-AU\left(t_{\mathrm{fin}} - t_{\mathrm{ini}}\right)/m_{\mathrm{S}} c_{\mathrm{pS}}} \tag{144}$$

For absorption:

$$T_{fin} = T_{w\,d} - \frac{\Delta H_{\mathrm{d}} r_{\mathrm{d}} m_{\mathrm{S}} SC}{AUMW_{\mathrm{MH}}} + \left(T_{\mathrm{ini}} - T_{\mathrm{wd}} + \frac{\Delta H_{\mathrm{d}} r_{\mathrm{d}} m_{\mathrm{S}} SC}{AUMW_{\mathrm{MH}}}\right) e^{-AU\left(t_{\mathrm{fin}} - t_{\mathrm{ini}}\right)/m_{\mathrm{S}} c_{\mathrm{pS}}} \tag{155}$$

Equations governing reaction kinetics and equilibrium pressure complete the model. These equations remain equal to those in the original model.

Comparison of simulation results of the model with differential equations and the model with just algebraic equations shows that there is an excellent match between the results of both models. The differences are so minimal that is not possible to perceive them in the graphics that shows the time evolution of variables. Therefore, the differences are determined analytically by calculating the maximal error between the models results. The maximal errors in the time evolution of the variables are the following:

System Temperature: 0.18%
System pressure: 2.01%
Material equilibrium pressure: 2.00%
Reaction rate: 0.52%
Hydrogen storage: 2.40%

As it can be seen, the error is not significant, showing the value and usefulness of the reduced model.

7. Conclusions

A simplified lumped model has been developed to study hydrogen thermal compression and storage processes that successfully reproduce numerical results and experimental measurements described in the literature. In the process engineering area, it is important to develop simplified models like this one, also called aggregated models, which can properly reproduce the occurring tradeoffs in real processes. These compromises can be more accurately represented by using much more complex rigorous models. However, if the aggregated model is able to reproduce the rigorous model results, its usefulness is remarkable in process design as well as in understanding the most important phenomena occurring within the process.

A cyclic process was presented that accomplishes common uses of hydrogen recovery and compression for metal treatment industries. This model allows simulating the process by varying key parameters in order to evaluate its performance

under different conditions, thus acquiring knowledge on the system behavior. This analysis proved the importance of the existing tradeoff in a complete absorption/heating/desorption/cooling cycle in relation to the convenience of stopping both absorption and desorption stages long before the hydride forming material is fully hydrided or dehydrided. Combining this approach with the reorganization of the cycle times would lead to a reduction of 25% or even more, in the amount of required hydrided forming material.

The implementation of sensitivity analysis as a powerful tool to evaluate changes in the design and operating conditions of a particular process has been described and exemplified. This study revealed the most important parameters when designing the process. The physicochemical properties of the material: enthalpy, entropy and the design parameter: cooling/heating water temperature, proved to be the most influential parameters in the performance of the cyclic process.

Finally, the constant reaction rate constraint was added and a further model simplification was achieved by integrating the ordinary differential equations. This simplification turned the differential and algebraic equations system into a just algebraic equations system. As a consequence of the simplification, the number of equations to be solved is reduced from over 15,000 to less than 50. The results of the simulations using both models are compared, showing that the maximal error in the time evolution of the variables is negligible. Therefore the usefulness of the model simplification is confirmed.

Acknowledgments

The authors acknowledge financial support provided by Consejo Nacional de Investigaciones Científicas y Técnicas (CONICET) and Agencia Nacional de Promoción Científica y Tecnológica (ANPCyT) of Argentina.

REFERENCES

[1] Wipf H, editor. Hydrogen in metals III (Topics in applied physics. Properties and applications). Berlin: Springer-Verlag; 1997.
[2] Forde T, Ness E, Yartys V. Modeling and experimental results of heat transfer in a metal hydride store during hydrogen charge and discharge. Int J Hydrogen Energy 2009;34:5121–30.
[3] Mayer U, Groll M, Supper W. Heat and mass transfer in metal hydride reaction beds: experimental and theoretical results. J Less-Common Metals 1987;131:235–44.
[4] Jemni A, Nasrallah S. Study of two-dimensional heat and mass transfer during absorption in a metal hydrogen reactor. Int J Hydrogen Energy 1995;20(1):43–52.
[5] Jemni A, Nasrallah S. Study of two-dimensional heat and mass transfer during desorption in a metal hydrogen reactor. Int J Hydrogen Energy 1995;20(11):881–91.
[6] Nasrallah S, Jemni A. Heat and mass transfer models in metal–hydrogen reactor. Int J Hydrogen Energy 1997;22(1): 67–76.
[7] Jemni A, Nasrallah S, Lamloumi J. Experimental and theoretical study of a metal–hydrogen reactor. Int J Hydrogen Energy 1999;24:631–44.
[8] Askri F, Jemni A, Nasrallah S. Study of two-dimensional and dynamic heat and mass transfer in a metal–hydrogen reactor. Int J Hydrogen Energy 2003;28:537–57.
[9] Demircan A, Demiralp M, Kaplan Y, Mat M, Veziroglu T. Experimental and theoretical analysis of hydrogen absorption in LaNi5–H2 reactors. Int J Hydrogen Energy 2005;30:1437–46.
[10] Satheesh A, Muthukumar P. Performance investigation of a double-stage metal hydride based heat pump. Appl Therm Eng 2010;30:2698–707.
[11] Satheesh A, Muthukumar P. Performance investigations of a single-stage metal hydride heat pump. Int J Hydrogen Energy 2010;35:6950–8.
[12] Satheesh A, Muthukumar P. Simulation of double-stage double-effect metal hydride heat pump. Int J Hydrogen Energy 2010;35:1474–84.
[13] Satheesh A, Muthukumar P, Anupam Dewan. Computational study of metal hydride cooling system. Int J Hydrogen Energy 2009;34:3164–72.
[14] Forde T, Maehlen JP, Yartys VA, Lototsky MV, Uchida H. Influence of intrinsic hydrogenation/dehydrogenation kinetics on the dynamic behavior of metal hydrides: a semi-empirical model and its verification. Int J Hydrogen Energy 2007;32:1041–9.
[15] Martin M, Gommel C, Borkhart C, Fromm E. Absorption and desorption kinetics of hydrogen storage alloys. J Alloys Comp 1996;238:193–201.
[16] Gambini M, Manno M, Vellini M. Numerical analysis and performance assessment of metal hydride-based hydrogen storage systems. Int J Hydrogen Energy 2008;33:6178–87.
[17] Mat M, Kaplan Y. Numerical study of hydrogen absorption in an Lm–Ni_5 hydride reactor. Int J Hydrogen Energy 2001;26:957–63.
[18] Nakagawa T, Inomata A, Aoki H, Miura T. Numerical analysis of heat and mass transfer characteristics in the metal hydride bed. Int J Hydrogen Energy 2000;25:339–50.
[19] Inomata A, Aoki H, Miura T. Measurement and modeling of hydriding and dehydriding kinetics. Int J Alloys Comp 1998; 278:103–9.
[20] Laurencelle F, Goyette J. Simulation of heat transfer in a metal hydride reactor with aluminium foam. Int J Hydrogen Energy 2007;32:2957–64.
[21] Rosenthal R. GAMS – a user's guide. Washington DC: GAMS Development Corporation; 2007.
[22] Muthukumar P, Venkata Ramana S. Numerical simulation of coupled heat and mass transfer in metal hydride-based hydrogen storage reactor. Int J Alloys Comp 2009;472:466–72.
[23] Muthukumar Prakash Maiya M, Srinivasa Murthy S. Experiments on a metal hydride-based hydrogen storage device. Int J Hydrogen Energy 2005;30:1569–81.
[24] Sandrock G. A panoramic overview of hydrogen storage alloys from a gas reaction point of view. J Alloys Comp 1999; 293–295:877–88.
[25] Suda S, Kobayashi N, Yoshida K. Reaction kinetics of metal hydrides and their mixtures. J Less-Common Metals 1980;73: 119–26.
[26] Krokos C, Nikolic D, Kikkinides E, Georgiadis M, Stubos A. Modeling and optimization of multi-tubular metal hydride beds for efficient hydrogen storage. Int J Hydrogen Energy 2009;34:9128–40.
[27] Marcovecchio M, Scenna N, Aguirre P. Improvements of a hollow fiber reverse osmosis desalination model: analysis of numerical results. Chem Eng Res Des 2010;88:789–802.